

Hydrothermal alteration at the Haib porphyry copper deposit, Namibia: Stable isotope and fluid inclusion patterns

J.M. Barr and D.L. Reid

Department of Geochemistry, University of Cape Town, Rondebosch 7700, Cape Town, RSA

Porphyry-type copper mineralisation is developed in a quartz-feldspar porphyry pluton of the 1900-1730 Ma Vioolsdrif Intrusive Suite, which crops out near the lower Orange River in southern Namibia. Petrographic evidence for hydrothermal alteration is widespread, but most intense in a zone near the central part of the elongate porphyry body. Both the porphyry and metavolcanic country rocks are affected. Potassic alteration that often characterises Phanerozoic porphyry-type copper mineralisation is difficult to distinguish in the Haib deposit because of the high-K nature of the calc-alkaline host rocks. Stable isotope patterns indicate depletion in ^{18}O (represented by low $\delta^{18}\text{O}$ whole rock and mineral values) and deuterium (low δD values) during hydrothermal alteration, which suggests the introduction and circulation of heated meteoric fluids. Preliminary studies have identified two types of fluid, an early high-salinity high-temperature fluid trapped in primary inclusions, and a late-stage low-temperature low-salinity fluid trapped as secondary inclusions in healed fractures.

Introduction

Copper in the Haib River area of southern Namibia (Fig. 1) was probably worked, like the richer Okiep deposits further south in Namaqualand, in pre-European times (Smalberger, 1975). There have been continuous reports from European prospectors describing the Haib copper showings since the early eighteenth century. Probably the biggest promotion of the Haib prospect commenced with its acquisition by the Swanson family interests just after World War 2. Since the 1950s, a number of exploration companies have examined the Haib prospect, with Rio Tinto Exploration (Pty) Ltd, who held rights to the deposit between 1972 and 1976, conducting the most comprehensive geological, geophysical and geochemical investigation. The deposit was extensively evaluated by diamond drilling and detailed geological mapping, which provided the basis and material for the current follow-up study.

Apart from many company reports prepared by Rio Tinto during its tenure at Haib, the company allowed

several university-based research programs to run concurrently with exploration (Blignault, 1977; Reid, 1977; Minnitt, 1979). These research results confirmed earlier assessments that the Haib deposit represented a well-preserved Precambrian example of an important class of copper deposit, the so-called porphyry-type, that is estimated to contain nearly 50% of the world's preserved of this strategic metal (Gustafson, 1978; Guilbert and Park, 1986). Estimated preserved of the Haib deposit are about one billion tonnes of very low grade copper ore (~0.1 - 0.2 % Cu), with traces of Mo and Au (Minnitt, 1986).

Another important feature of the Haib is the lack of overburden covering the ore zone, which is due to the arid climate and highly dissected terrain near the canyon of the lower Orange River. A well-developed oxidised capping is present at surface and has potential for low-cost exploitation using combined heap-leaching, electro-winning technology, prior to longer term open pit mining of the deeper seated primary sulphide ore. Recent high copper prices on the world market, political developments in Namibia, dwindling preserved at established underground mines such as Okiep and Tsumeb, have resulted in renewed interest in the Haib deposit.

Much detailed regional and local mapping of the Haib porphyry deposit has already been carried out (Blignault, 1977; Minnitt, 1986), while the 50+ km of diamond drill core recovered by Rio Tinto is still in good condition and maintained at the prospect by Swanson Enterprises (Pty) Ltd. It was considered opportune to carry out a detailed follow-up study, concentrating on geochemical aspects of the porphyry-style hydrothermal alteration that is responsible for the copper mineralisation. Of special significance was the great age of the deposit (~1800 Ma; Reid, 1979a), which sets it apart from the majority of producing porphyry systems, which are Mesozoic to Tertiary in age (Guilbert and Park, 1986).

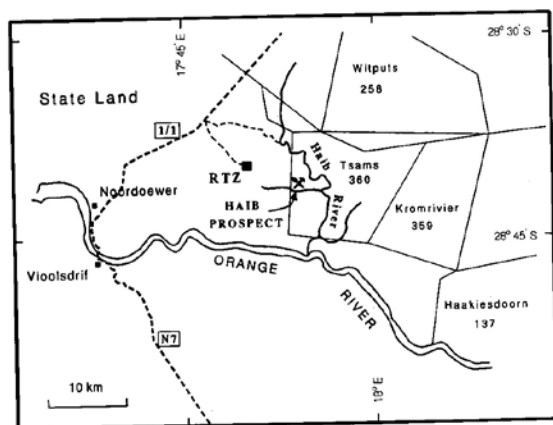


Figure 1: Location of the Haib Porphyry Copper Deposit (HPC)

Geological Setting

Porphyry-style copper mineralisation is developed in and around a quartz-feldspar porphyry (hereafter QFP) intrusion, which is a minor phase of a large composite batholith formed by plutons of the Vioolsdrif Intrusive Suite (VIS). The VIS intrudes its broadly coeval volcanic roof, which comprises lavas, tuffs and volcanoclastic sediments of the Haib Volcanic Subgroup (HVG). Situated in the mountainous terrain that straddles the lower Orange River between Namibia and South Africa (Fig. 1), the study area is underlain by a series of roughly east-west-trending belts of volcanic and plutonic rocks (Fig. 2). Such an outcrop pattern reflects the tendency for the east-west fold axes developed in the HVG to control the emplacement of the VIS plutons. The Haib QFP also reflects this structural influence and has an extreme aspect ratio quite unlike the text-book examples of circular plutons surrounded by annular zones of progressive alteration and mineralisation. While showing some alteration throughout, the main zone of alteration and mineralisation occurs roughly in the central part of the elongate body (Fig. 2).

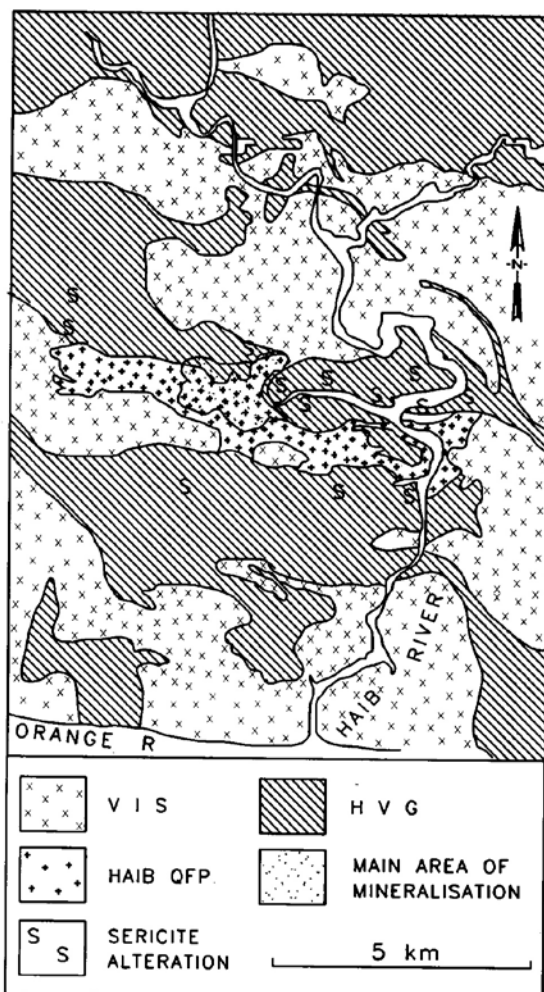


Figure 2: Geological sketch map of the area around the Haib prospect (after Blignault, 1977; Minnitt, 1986)

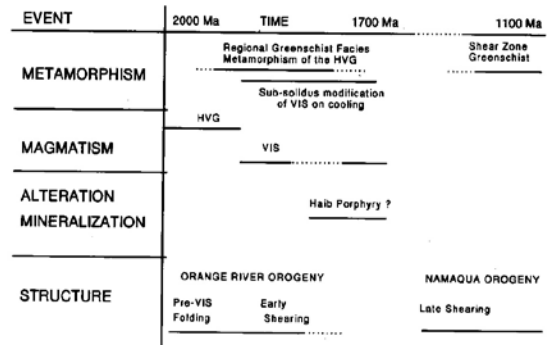


Figure 3: Summary of the geological history of the Haib area

The geological history of the Haib region is summarised in Figure 3, where it is suggested that volcanism and plutonism occurred within an active tectonic setting, during which early lavas and tuffs were folded and metamorphosed prior to intrusion of the granitoid plutons (Blignault *et al.*, 1983). Early plutons were themselves deformed prior to emplacement of younger ones, so there is a direct relationship between age of emplacement and degree of deformation and metamorphism. Radiometric dating of the HVG indicates eruption ~ 2000 Ma ago (Reid, 1979b).

Detailed petrographic studies and radiometric dating have revealed the composite nature of the VIS, which involves emplacement of progressively more felsic rock types with time (Reid, 1979a; 1982). There also appears to be a distinct hiatus in intrusion between the more mafic granitoids (diorite, tonalite, granodiorite) at 1900 ± 30 Ma, and the more felsic granitoids (monzonite, adamellite, leucogranite) at 1730 ± 20 Ma. The Haib QFP did not yield a precise Rb-Sr age and its bulk composition is transitional between the older Vioolsdrif granodiorites and younger adamellites (Reid, 1977; Minnitt, 1986). Field evidence does however indicate that the Haib QFP intrudes granodiorites in the study area, and is itself intruded by small bodies of leucogranite, suggesting emplacement at a late stage in the history of the VIS.

There is also evidence that hydrothermal alteration and sulphide mineralisation of the Haib QFP took place after a regional greenschist facies metamorphic event (Fig. 3). Quartz-sulphide veins crosscut the S_1 axial-planar foliation in the tightly folded metavolcanic country rocks, the foliation being defined by a greenschist facies mineral assemblage. The chlorite-sericite alteration assemblage represents a hydrothermal retrogression of the biotite-albite-quartz-epidote greenschist facies metamorphic assemblage. Hydrothermal chlorite also partly replaces elongate crystals of metamorphic actinolite in some of the more basic lavas. Also, in some rocks hydrothermal chlorite has pseudomorphed a metamorphic porphyroblastic mineral, which might have been garnet, although no remnant grains have been recognised.

Reid (1977) attributed this early metamorphic episode to a regionally developed thermal metamorphism occurring upon emplacement of the VIS. A second greenschist facies metamorphic event that is younger than the Haib QFP and all the Vioolsdrif granitoids, is restricted to narrow shear zones that ramify the Haib area. In places the Haib QFP has developed a slight foliation in response to this late shearing. In their regional study, Blignault *et al.* (1983) attributed these late shears to the ~1100 Ma Namaqua tectonothermal event. Reid (1982) also noted that the latter event caused mineral-scale overprinting of the Rb-Sr radiometric system throughout the Haib area. In summary, the Haib porphyry system developed in a pluton that had intruded already metamorphosed country rock, and was itself mildly metamorphosed and deformed during later events.

Petrography

The two rock types that host the mineralisation at the Haib prospect are the intrusive QFP and its adjacent country rock which consists mainly of feldspar-phyric lavas (here referred to as feldspar porphyry or FP). Brief petrographic descriptions of these two rock types are given below in order to illustrate the petrographic evidence for hydrothermal alteration.

Quartz-feldspar porphyry

The QFP is the main host to the mineralisation at the Haib prospect and field relationships show it to have intruded the FP with sharp contacts. Xenoliths of FP are not uncommon in the QFP. The QFP is a fine-grained to medium-grained, holocrystalline rock that is usually porphyritic but is sometimes equigranular. Phenocryst minerals include plagioclase and bluish opalescent quartz which together may make up 40% by volume of the rock. Rare alkali feldspar and biotite phenocrysts also occur. The average phenocryst size is 1-2 mm.

The groundmass consists of quartz, plagioclase, alkali feldspar and chloritised biotite and is seriate to equigranular in texture. Variations in matrix grain size, mafic mineral content, alkali feldspar and plagioclase content and a locally developed weak foliation give the intrusion a complex petrographic character. Modal analyses show the QFP to be intermediate between the granodiorites and adamellites in the region.

The QFP is a minor constituent of the VIS, the only other occurrences being the Tatasberg prospect in the northeast Richtersveld (De Villiers and Söhnge, 1959; Blignault, 1977), and the Lorelei prospect (Viljoen *et al.*, 1986). Whereas apparently unmineralised quartz feldspar porphyry bodies occur near Nous Wells (Reid, 1977), base metal (Cu, Mo) mineralisation is associated with hydrothermal alteration of Vioolsdrif granitoids (other than obvious porphyry rock types), e.g. the Krom River and Xamchab leucogranites (Minnitt, 1979; Von Backstrom and De Villiers, 1972). The latter prospect

also contains appreciable scheelite mineralisation (Bowles, 1988) and also apparently yielded a nugget of gold (Gevers *et al.*, 1937).

Feldspar porphyry

Massive and jointed porphyritic metalavas constitute the country rock to the Haib QFP and range in chemical composition from andesite to rhyodacite (Reid 1979c). Since these compositional features are not easily discernible in the field, the entire package was mapped as "feldspar porphyry" or FP. The phenocryst assemblage consists of subhedral, pale green saussuritised plagioclase and mafic aggregates of biotite-chlorite-epidote-sphene after biotite, augite, orthopyroxene and possibly amphibole. Compositional zoning of the plagioclase phenocrysts controls the distribution of the secondary epidote within the pseudomorphs. More felsic types also contain quartz phenocrysts with subhedral embayed outlines. The matrix is dark coloured and fine-grained and consists of a granular recrystallised mosaic of biotite, chlorite, epidote, muscovite, quartz and feldspar. Both the recrystallised texture of the ground-mass and abundance of secondary minerals replacing the primary igneous assemblage point to the lavas being metamorphosed to upper greenschist facies grade (Reid, 1977; Van Aswegen, 1988).

Alteration

Metamorphic reconstitution of the metavolcanic country rock has already been described. Granitoid rocks of the VIS in the Haib area invariably contain sericitised and saussuritised plagioclase and primary, coarse, brown biotites has been partly replaced by secondary green biotite and chlorite. In the more basic plutons (tonalite, granodiorite) secondary biotite has pseudomorphed euhedral amphibole. Epidote and carbonate veins, often with marginal zones of alteration, are widespread throughout the granitoids. Near shear zones the rocks are recrystallised to gneisses or even schists, with replacement of large subhedral grains of biotite by trains of small biotite flakes and epidote parallel to the foliation.

Minnitt (1979) interpreted the regionally developed greenschist facies mineralogy of the HVG as propylitic hydrothermal alteration, associated with the emplacement of the Haib porphyry. Biotite developed throughout the HVG in this area, as well as the K-feldspar and biotite developed in the Haib porphyry itself, was considered to be a product of potassic hydrothermal alteration, in the sense that potassium had been introduced. On a more regional scale, Reid (1979c) was able to demonstrate that the HVG was a high-K calc-alkaline suite, which was characterised by the presence of K-feldspar and biotite in the groundmass of the more felsic members. These two minerals also occur as phenocrysts in some of the rhyolites. Widespread potas-

sium metasomatism of the volcanic sequence can be ruled out. Furthermore, metamorphic recrystallisation of such potassic lavas has resulted in the appearance of secondary.

K-feldspar and biotite in the groundmass of even more basic types (basaltic andesite, andesite). Compounding the problem is the recognition of two distinct greenschist facies metamorphic episodes, both of which could have generated K-feldspar and biotite. Burnham (1962) has already highlighted the similarity between potassium silicate alteration and the mineral facies typical of most granites. Probably the only situation where such potassic alteration can be easily recognised would be intrusive suites that crystallised under low P_{H_2O} where deuteric alteration is not prevalent, or in low-K granitoids and their porphyritic counterparts.

In spite of the difficulties in distinguishing low-grade metamorphic reconstitution from hydrothermal alteration, it is still possible to discern those petrographic features that are unequivocally due to the latter in the vicinity of the Haib QFP. Minnitt (1986) identified the three silicate mineral alteration assemblages that are present at the Haib prospect: (1) potassium silicate, (2) chlorite-sericite and (3) quartz-sericite. The intrinsic K-rich nature of the Haib QFP argues against it having experienced a high degree of pervasive potassium-silicate alteration, as suggested by Minnitt (1986).

Localised potassium-silicate alteration of the Haib QFP does occur, generally forming haloes around veins and is characterised in hand specimen by a deep red colouration of the rock. Wenner and Taylor (1976) reported a similar brick red colouration of feldspars in the Proterozoic (1400-1500 Ma) St Francois Mountains Batholith, Missouri, and concluded that it is caused by oxidation of Fe originally in the feldspar lattice and its subsequent appearance as finely divided hematite, in response to a hydrothermal alteration event. Microscopic examination of rocks from the Haib prospect reveal the growth of small, anhedral secondary microcline and orthoclase crystals which contain abundant inclusions of matrix minerals. Alkali feldspar also occurs in small veins, which sometimes cut through quartz phenocrysts, and within larger veins with quartz and calcite. Ferry (1985) has shown for the Skye granites that hydrothermally altered alkali feldspar has a wider range in composition (Na/K ratio) than primary igneous grains. It should therefore be possible to determine the true extent of potassium silicate alteration at the Haib by looking at differences between alkali-feldspar compositions in altered and unaltered zones.

Chlorite-sericite alteration is widespread in the QFP and FP around the Haib intrusion, its borders approximating the zone of main mineralisation (Fig. 2). Although the igneous porphyritic texture is preserved with this type of alteration there is extensive mineralogical reconstitution. Biotite is replaced along cleavage traces by chlorite and continued alteration has led to complete replacement by small flakes of chlorite. The end-

product of this type of alteration of biotite is anhedral patches of chlorite with some sericite. Plagioclase is intensely sericitised, but alkali feldspar is relatively fresh. Disseminated sulphide may occur within the patches of altered mafic silicates.

Quartz-sericite alteration at Haib is intense, almost completely destroying the igneous texture, and is developed both in the QFP and FP. Recrystallised quartz phenocrysts and sericite pseudomorphs after plagioclase are occasionally discernible. The mineralogy is dominantly quartz and sericite, with minor tourmaline mineralisation. There may have been two generations of phyllic alteration, with the earlier phase being related to fumarolic activity at the time of lava extrusion and recognised by the same fabric that is developed in the surrounding unaltered metavolcanic rocks. The later phase, related to the Haib QFP, has produced unfoliated zones of altered rock whose margins are generally discordant to any foliation in the surrounding rocks. These white alteration bodies define a patchily developed phyllic alteration halo around the QFP (Fig. 2). Quartz-sericite alteration of the type encountered at Haib is not known from any other locality.

Analytical methods

Oxygen isotope analyses were performed at the University of Cape Town using methods described in Venemann and Smith (1990). All mineral and whole-rock samples were run in duplicate and normalised to a value for NBS-28 of 9.64‰. Isotope ratios are reported in the standard delta notation relative to Vienna Standard Mean Ocean Water (V-SMOW). Analytical uncertainties are estimated as 0.02‰ for minerals and 0.05 K for whole rocks.

Hydrogen isotope analysis of whole rocks and biotite were carried out at the University of Michigan. H_2O recovered from samples heated in a furnace to 1350°C

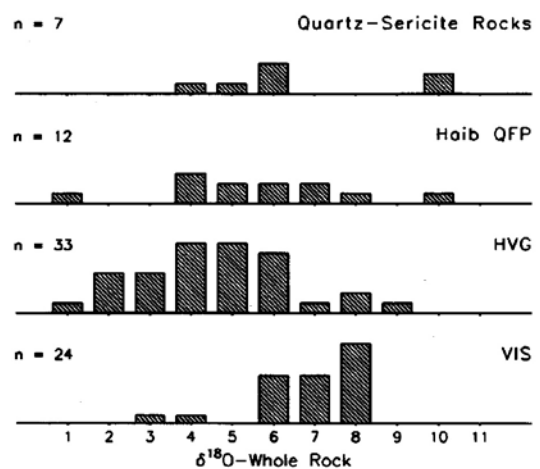


Figure 4: Histogram of $\delta^{18}O$ data for various rock types encountered in and around the Haib area

SAMPLE	DESCRIPTION	$\delta^{18}\text{O}$ ‰	SAMPLE	DESCRIPTION	$\delta^{18}\text{O}$ ‰
<i>Haib area</i>			<i>Regional Samples from Reid (1977)</i>		
HB047 (155)	QFP from main mineralised area	3.6	DRS-20	peridotite	3.3
HB010 (11)	QFP	9.1	DRS-100	troctolite	6.2
JB 109	QFP from eastern end of intrusion	6.4	DRS-83	gabbro	6.6
RT-02	QFP	6.4	DRV-08	diorite	6.9
RT-03	QFP	7.4	DRV-63	diorite	6.8
DRP-01	QFP	3.9	DRV-08C	diorite	7.2
DRP-01A	QFP	3.7	DRV-50	tonalite	7.7
DRP-02	QFP	5.7	DRV-44	tonalite	6.0
HB004 (77)	FP (andesite)	4.3	DRV-55	tonalite	2.9
DRP-04	FP (andesite)	4.6	DRV-75	tonalite	7.3
DRP-10	FP (andesite)	3.1	DRV-09	granodiorite	7.6
DRP-12	FP (andesite)	4.2	DRV-15	granodiorite	6.4
JB 113	FP (andesite)	2.0	DRV-01	adamellite	7.3
JB 115	FP (dacite)	8.3	DRV-22	leucogranite	7.6
JB 88	FP (rhyolite)	5.8	DRV-12B	leucogranite	5.4
JB 104	FP (rhyolite)	6.4	DRV-58	leucogranite	7.8
JB 105	diorite	5.8	DRL-55	rhyolite	7.8
JB 68	granodiorite	7.2	DRL-67	basaltic andesite	4.6
JB 102	foliated adamellite	5.5	DRL-70	andesitic tuff	4.0
JB 106	leucogranite	7.3	DRL-71	dacite	4.9
DRL-78C	andesite	0.6	DRL-74	basaltic andesite	2.1
DRL-81	basaltic tuff	1.6	DRL-76	rhyolite	5.2
DRL-73	andesite	5.4	DRL-78A	dacite	5.1

Table 1: Whole-rock $\delta^{18}\text{O}$ data for volcanic and plutonic rocks from the Haib area. Samples prefixed HB- are from diamond drill core: borehole no., followed by depth in metres in brackets

was converted to H_2 by reaction with Zn at 500°C. D/H ratios are reported in conventional delta notation relative to SMOW. Values of δD obtained for the NBS-30 standard were in the range $-63 \pm 1\%$, compared with the reference value of -64.5% . Estimated uncertainty in the δD data is $\pm 0.5\%$.

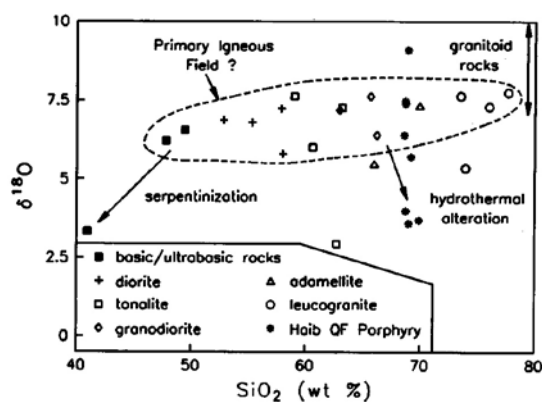


Figure 5: Plot of $\delta^{18}\text{O}$ versus SiO_2 content in samples from the Vioolsdrif Intrusive Suite (VIS) and the Haib Quartz-Feldspar Porphyry (QFP)

The fluid inclusion analyses were done on a modified USGS gas flow heating/freezing stage marketed by Fluid Inc. (e.g. Reynolds and Beane, 1985), installed on a Leitz microscope in the Department of Geology, University of the Witwatersrand. Doubly polished mineral slices were prepared at UCT and fluid inclusions mapped and characterised prior to microthermometric analysis so that heating and freezing could be performed on the same inclusions.

Stable isotope Patterns

Whole-rock oxygen isotope data

The $\delta^{18}\text{O}_{\text{wr}}$ values for different rock types in the Vioolsdrif Intrusive Suite and Haib Subgroup are given in Table 1. Apart from samples from the Haib area, a more regional collection of intrusive and extrusive rocks (that of Reid, 1977) was also analysed for comparative purposes. Four suites are compared by means of histograms in Figure 4. Granitoids of the VIS have $\delta^{18}\text{O}$ mostly between 6 and 8‰, while a much wider range in $\delta^{18}\text{O}$ is displayed by both the HVG and Haib QFP. Rocks affected by quartz-sericite alteration also

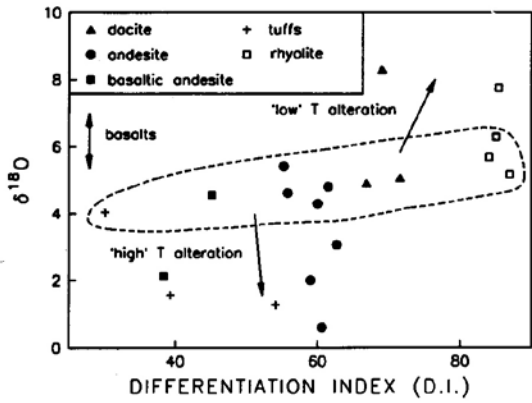


Figure 6: Plot of $\delta^{18}\text{O}$ versus Differentiation Index (Thornton and Tuttle, 1960) for samples from the Haib Volcanic Subgroup (HVG)

show a range, but the majority have relatively low $\delta^{18}\text{O}$ values.

Figure 5 shows the variation between the $\delta^{18}\text{O}$ values obtained in this study with SiO_2 data from Reid (1977). Samples ranging in composition from gabbro to granite plot in a narrow $\delta^{18}\text{O}$ range (6-7.5 ‰) and resemble primary magmatic values. For example, basaltic rocks formed from mantle-derived magmas have $\delta^{18}\text{O}$ between 5 and 6 ‰ (Keyser, 1986). Limited variation in $\delta^{18}\text{O}$ (about 1 ‰) with differentiation is expected and the observed range for the majority of granitoid samples shown in Figure 5 could be regarded as defining a primary igneous field. Samples plotting below the primary igneous field appear to have experienced depletion in ^{18}O .

A serpentinised peridotite (sample DRS-20 in Table 1) has a very low $\delta^{18}\text{O}$ of 3.3 ‰, which is probably the result of exchange with meteoric water during the serpentinisation process (e.g. Ikin and Harmon, 1984). The salient feature of Figure 5 is probably the wide variation in $\delta^{18}\text{O}$ shown by the Haib QFP. For a limited range

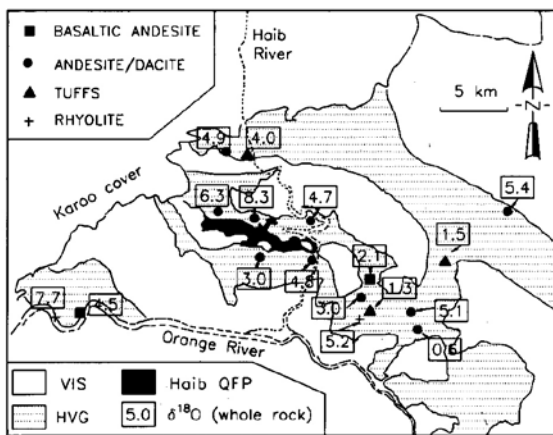


Figure 7: Regional variation in $\delta^{18}\text{O}$ values for the HVG

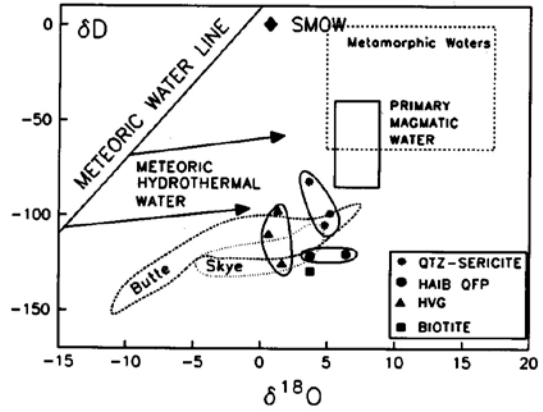


Figure 8: Plot of δD versus $\delta^{18}\text{O}$ for selected whole rocks and a biotite separate from the Haib area. Fields are indicated for magmatic, meteoric and metamorphic waters. Fields occupied by altered plutonic and volcanic rocks from Skye and the Butte ore district (including Nevada) are after Criss and Taylor (1986) and Sheppard (1986)

in SiO_2 , the Haib QFP samples have $\delta^{18}\text{O}$ values ranging from a high of 9.1 ‰ (above the primary igneous field) down to 3.7 ‰. Clearly the altered rocks from the Haib QFP have been severely disturbed, with the observed pattern suggesting open system exchange with fluids characterised by low $\delta^{18}\text{O}$. Depletion in ^{18}O is not confined to the Haib QFP pluton, as one tonalite (DRV-55, southeast of Violsdrif) and one leucogranite (DRV-12B, from the lower Haib River area), also have low $\delta^{18}\text{O}$. Both samples show advanced propylitic alteration.

The $\delta^{18}\text{O}$ data for metavolcanic rocks of the Haib Subgroup are listed in Table 1 and plotted against Differentiation Index (D.I., Thornton and Tuttle, 1960) in Figure 6. Adopting the same procedure applied to the granitoids by defining a field occupied by the majority of the data points enables the recognition of alteration effects. However, the field outlined in Figure 6 is displaced to lower $\delta^{18}\text{O}$ when compared with the primary igneous field defined for the granitoids. Even the use of previously published ranges in $\delta^{18}\text{O}$ for basaltic rocks highlights the relative depletion in ^{18}O . Apart from some andesite and dacite samples with $\delta^{18}\text{O}$ in the range of 5-6 ‰, few of the metavolcanic rocks appear to have retained their primary igneous signature. Vectors indicating the expected changes in $\delta^{18}\text{O}$ during certain types of hydrothermal alteration are shown in Figure 6 for reference. High-temperature exchange with heated meteoric waters tends to cause depletion in ^{18}O , and most of the analysed samples seem to have experienced such a process. Low-temperature alteration involves the deposition of secondary minerals characterised by very high $\delta^{18}\text{O}$, caused by the large isotope fractionation factors. Only two of the analysed samples appear to have been affected by this latter process.

It is difficult to establish whether this low temperature process could be equated with a period of super-

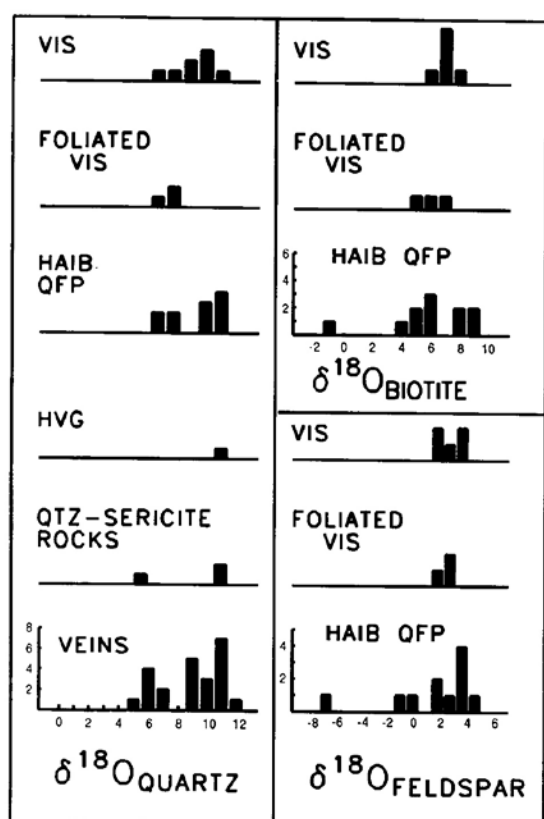


Figure 9: Histogram of $\delta^{18}\text{O}$ -mineral values (quartz, feldspar and biotite) from different rock types encountered in and around the Haib area

gene activity. Very little easily recognisable supergene modification (e.g. a secondary "chalcocite blanket") can be observed. There is however an extensive zone of oxidation, generally restricted to the upper 10-20 metres below surface, which is recognisable in many exploration boreholes. While this oxidation zone was specifically avoided during the present sampling study,

it is possible that samples with high $\delta^{18}\text{O}$ could be reflecting this surface effect. It would be an interesting extension of the present study to focus more attention on the near-surface oxidation zone, especially in view of current interest in its economic potential.

While many of the metavolcanic samples with low $\delta^{18}\text{O}$ are located near the Haib QFP, there does not seem to be a consistent pattern of ^{18}O depletion. All the samples analysed are plotted on a locality map in Figure 7, showing their distribution relative to the Haib QFP. Samples from adjacent outcrops may differ considerably in $\delta^{18}\text{O}$ (eg. DRL-78A: 5.1 ‰, DRL-78C: 0.6 ‰). Clearly the process of ^{18}O depletion has been confined to discrete zones, possibly controlled by channelled rather than pervasive fluid flow. In addition, the ^{18}O depletion observed throughout the HVG, as shown in Figure 7, is possibly also the product of hydrothermal systems that accompanied the emplacement and cooling of the many other granitoid plutons that make up the batholith.

Hydrogen isotope data

D/H ratios (expressed as δD values) determined for selected whole-rock samples and a biotite separate are listed in Table 2 and plotted against $\delta^{18}\text{O}$ in Figure 8. All analysed samples including the biotite are depleted in deuterium (and to a lesser extent ^{18}O) relative to data typical of igneous and metamorphic rocks recorded by Sheppard (1986). Admixtures of meteoric with magmatic (or metamorphic) waters are illustrated in Figure 8 by vectors emanating from the meteoric water line. Judging from the distribution of data points, H_2O fixed in the Haib rocks (and biotite) could be explained as a mixture of magmatic and highly deuterium-depleted meteoric water. In terms of modern analogues, meteoric water with δD of -100 to -150 ‰ is typical of high latitudes.

Sample	Rock Type	Weight (mg)	δD ‰-SMOW	wt % H_2O
JB 95	Qtz-Sericite	38.87	-105.4	1.97
		38.25	-104.9	2.02
JB 91	Qtz-Sericite	46.63	-82.1	1.85
JB 110	Qtz-Sericite	40.33	-98.9	1.79
DRL-78C	Andesite	53.75	-109.7	1.60
DRL-77	Andesitic Tuff	48.33	-97.2	1.45
DRL-81	Basaltic Tuff	58.79	-125.3	1.38
		36.55	-125.7	1.35
DRP-01A	Haib QFP	50.43	-121.6	1.15
RT-02	Haib QFP	53.27	-120.5	1.07
JB 105	Diorite (Biotite)	17.52	-129.6	3.18

Table 2: Hydrogen isotope data for whole-rock samples and biotite separates

SAMPLE	DESCRIPTION	$\delta^{18}\text{O}$ - MINERAL ‰		
		QUARTZ	FELDSPAR	BIOTITE
HB 010 (134)	QFP with deep red colouration	9.7	8.5	3.1
HB 019 (184)	QFP	10.8	7.3	3.2
HB 031 (292)	QFP	6.5	5.0	-0.7
HB 034 (286)	QFP	10.4	5.9	3.8
HB 035 (312)	QFP	7.5	-1.4	-7.0
HB 060 (307)	QFP	9.6	3.3	-1.1
HB 062 (80)	QFP	9.5	7.4	3.9
HB 092 (118)	QFP	10.4	8.7	4.6
HB 095 (386)	QFP	6.7	5.6	1.1
HB 105 (317)	leucocratic QFP	10.6	4.7	2.1
JB 44	northern granodiorite	7.0	6.3	1.5
JB 56	foliated adamellite	6.4	5.6	2.2
JB 68	northern granodiorite	9.6	7.3	2.9
JB 76	northern granodiorite	9.0	7.0	3.9
JB 105	diorite	8.8	6.9	3.7
JB 106	leucogranite	7.5	6.9	-
JB 108	foliated adamellite	7.5	6.6	2.3
JB 109	QFP from eastern end of intrusion	7.8	5.7	1.5
JB 118	QFP from eastern end of intrusion	7.5	4.4	1.8
JB 123	southern granodiorite	9.6	5.2	1.6

Table 3 (above): $\delta^{18}\text{O}$ data for mineral separatesTable 4 (below): Oxygen isotope temperatures ($^{\circ}\text{C}$) calculated for coexisting mineral pairs

SAMPLE	DESCRIPTION	QUARTZ-FELDSPAR	QUARTZ-BIOTITE	FELDSPAR-BIOTITE
JB 44	northern granodiorite	1109	480	355
JB 68	northern granodiorite	478	413	381
JB 76	northern granodiorite	534	506	491
JB 105	diorite	618	506	445
JB 106	leucogranite	1072	-	-
JB 123	southern granodiorite	263	357	443
DRV 01	adamellite	350	-	-
DRV 58	leucogranite	506	-	-
HB 010 (134)	QFP	735	418	335
HB 019 (184)	QFP	307	373	418
HB 031 (292)	QFP	626	390	320
HB 034 (286)	QFP	236	418	646
HB 035 (312)	QFP	81	196	325
HB 060 (307)	QFP	153	273	396
HB 062 (80)	QFP	483	476	471
HB 092 (118)	QFP	570	461	418
HB 095 (386)	QFP	781	473	389
HB 105 (317)	QFP	168	339	569
JB 109	QFP	483	433	410
JB 56	foliated adamellite	1018	579	461
JB 108	foliated adamellite	943	499	388
JB 118	foliated adamellite	371	467	550

The fields occupied by the Haib rocks are similar to those established for many hydrothermally altered igneous complexes emplaced at high palaeo-latitudes, such as the Skye granites, Idaho batholith and Skaergaard intrusion (Criss and Taylor, 1986). More critical perhaps is the overlap with fields occupied by several ore deposits, where the mineralisation is considered to accompany hydrothermal activity. Examples shown in Figure 8 include the Butte and

Nevada ore districts (Criss and Taylor, 1986). The displacement from the meteoric water line indicates high degrees of water/rock interaction, in order to produce the isotopic shift.

Oxygen isotope data on mineral separates

Oxygen isotope data for quartz, feldspar and biotite separated from rocks of the VIS and Haib QFP are listed in Table 3. Comparison of the various rock types investigated is made in Figure 9 in the form of histograms. The Haib QFP has a range of values that is greater than that of the VIS (including the foliated rocks). This increased variability in $\delta^{18}\text{O}$ values is more marked for feldspar and biotite than for quartz. At a fairly advanced stage of mineral exploration a knowledge of the variability of $\delta^{18}\text{O}$ values of minerals from a single pluton may be of use in identifying potentially well-mineralised intrusions. The predicted sequence of ^{18}O enrichment (quartz > feldspar > biotite), is followed by the present results, and no isotopic reversals have been encountered.

Coexisting mineral pairs for which $\delta^{18}\text{O}$ data are available have been plotted in a series of diagrams (Fig 10a-c). For mineral pairs to be in oxygen isotope equilibrium, the data points must follow a line of constant Δ . Inspection of the Quartz-Feldspar (Fig. 10a) and Quartz-Biotite (Fig. 10b) plots reveals that these mineral pairs show marked disequilibrium. Values for Δ vary widely and translate to an impossible range of calculated isotope temperatures (Table 4). On the other hand, a more coherent pattern is displayed by the Feldspar-Biotite plot (Fig. 10c), where the limited range in Δ values translates to perhaps more realistic estimates of temperature. The patterns suggest that feldspar and biotite continued to exchange oxygen isotopes between each other and a hydrothermal fluid after quartz became closed. Alternatively, the two minerals could be the product of lower temperature potassium silicate alteration.

Oxygen isotope temperatures for the three mineral pairs have been calculated (Table 4) using fractionation factors obtained from the literature (Table 5). As would be predicted from the plots in Figure 10a-c, wide ranges in temperatures have been obtained. A better idea of the temperature patterns is obtained from Figure 11, where the three mineral pairs are compared on histograms. Quartz-feldspar temperatures show a large variation and are probably meaningless. Less scatter is apparent

in the quartz-biotite and feldspar-biotite temperatures and both mineral pairs yield the same mean temperature of $\sim 430^\circ\text{C}$.

The $\delta^{18}\text{O}$ values of quartz separated from veins are listed in Table 6, and range from +7 ‰ to +10.4 ‰. Assuming a $\delta^{18}\text{O}$ value for water in equilibrium with quartz of 0 ‰ (strong meteoric component), and applying the quartz-water oxygen isotope fractionation factors summarised in Table 5, a geologically feasible temperature range of 245DC to 345°C is indicated for vein quartz deposition.

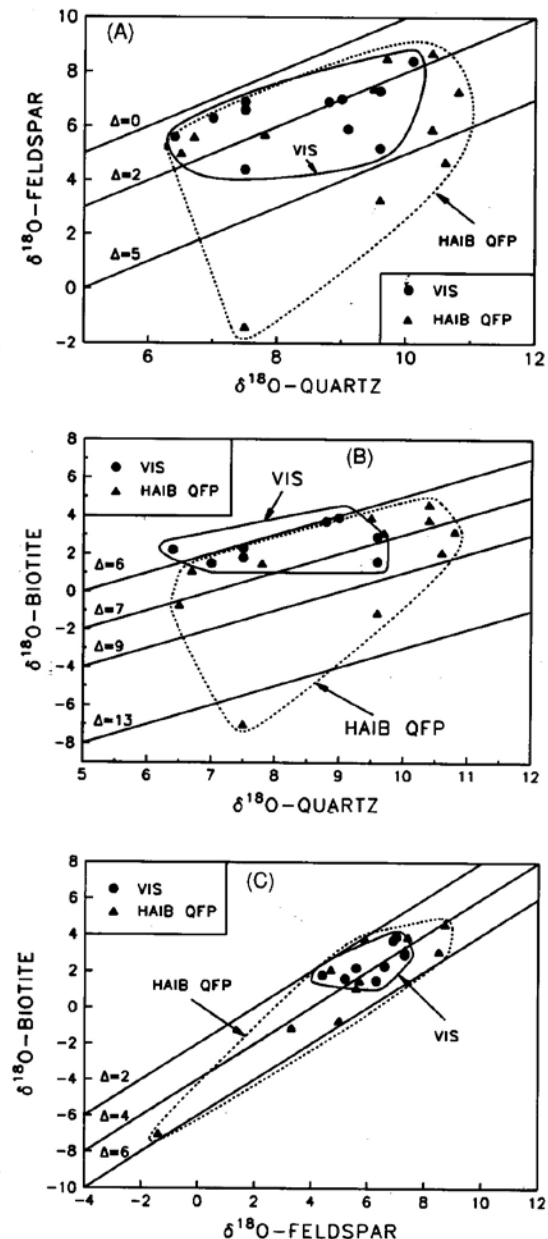


Figure 10: Plot of $\delta^{18}\text{O}$ data for coexisting mineral pairs (A) Quartz - Feldspar (B) Quartz - Biotite (C) Feldspar - Biotite The values correspond to $\delta^{18}\text{O}_{\text{min}1} - \delta^{18}\text{O}_{\text{min}2}$

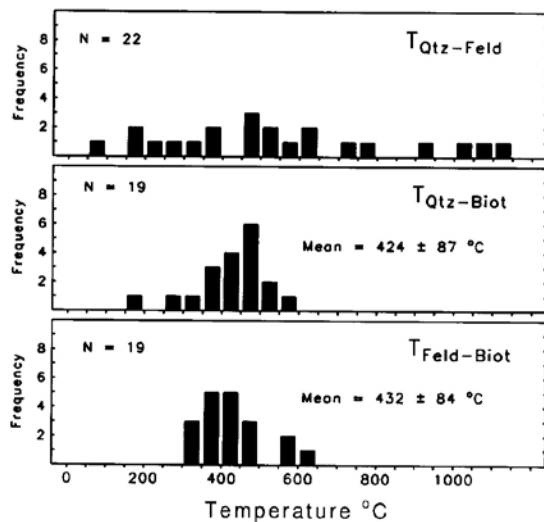


Figure 11: Histograms of oxygen isotope temperatures for the three mineral pairs investigated

Fluid Inclusions

The study of fluid inclusions in rocks and minerals from the Haib is still underway and only preliminary data are reported and discussed here. Fluid inclusions in quartz from a 1-cm-thick quartz-sulphide-calcite vein (sample HB004 (123)), which cuts through the FP host rock within the main mineralised area, have been investigated. Three types of inclusion have been recognised

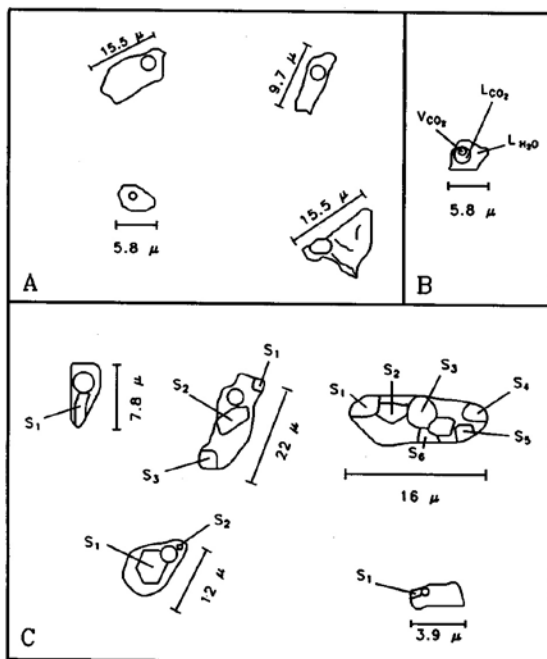


Figure 12: Sketches of the various types of fluid inclusion present in quartz from a vein cutting the country rock to the Haib QFP in the main mineralised area. Type A and B inclusions contain only liquid plus vapour bubbles, while type C inclusions contain solids (labelled S₁, S₂, etc), as well as liquid and vapour bubbles

within this sample and are illustrated in Figure 12. At room temperature type A comprise two phase (liquid + vapour) aqueous inclusions with a wide range of morphologies and sizes. Type B are three-phase “double bubble” inclusions (liquid CO₂, vapour CO₂ and liquid H₂O), while Type C are inclusions containing solid phases as well as liquid and vapour H₂O. Some of the solids in Type C inclusions may be daughter salts but others may be solid particles (perhaps quartz?) that were carried in the fluid. Of the three types, only C could be primary, while A and B are probably secondary inclusions, representing late-stage fluids trapped in annealed fractures.

Compositional data from freezing the two-phase Type A inclusion's are presented in Table 7 and Figure 13. Six out of 23 inclusions examined gave reproducible first melting temperatures (T₁), interpreted as eutectics, and it appears that the solutions approximate to the NaCl-H₂O system, perhaps with some KCl present. The T_m (final melting temperature) shows a skewed distribution ranging from -0.8°C to -4.3°C (Fig. 13), with an average value of -2°C which corresponds to 3.37 wt % equivalent NaCl. One inclusion with a eutectic T_m of -15°C might have magnesium chloride present. More data are needed before a statistically valid interpretation can be made.

Homogenisation temperatures (T_h) for 45 Type A and three Type C inclusions are presented in Figure 14. All the Type A inclusions homogenised into the liquid, while the Type C inclusions homogenised into the liquid with the solid phases still present. Values for T_H range from 170°C to 330°C and this wide range may be due to post-entrapment modification of the inclusions possibly at the time of measurement. Again more data are required for a statistically valid interpretation but the data do possibly represent a single generation of fluid homogenising at around 250°C. The trapping temperature can be up to 200°C higher depending on the pressure of entrapment. Complete dissolution of solid phases in Type C inclusions was not achieved, although some of the solids commenced dissolution by 490°C. One Type B inclusion was examined, the CO₂ homogenised at 27.8°C but the CO₂-H₂O had still not homogenised by 480°C.

Discussion

Results obtained thus far in this geochemical study of the Haib porphyry copper deposit have confirmed the existence of discrete zones of hydrothermal alteration associated with the mineralisation, as described originally by Minnitt (1986). It is, however, evident that the metavolcanic country rock around the Haib porphyry was already metamorphosed to greenschist facies prior to intrusion and the hydrothermal fluids interacted with a metamorphic, rather than an igneous, mineral assemblage. The high- K character of both the volcanic rocks of the HVG and the granitoids of the VIS makes

$\Delta = 10^3 \ln \alpha = A \times 10^6 / T^2 + B$ (Bottinga and Javoy, 1974)

MINERAL PAIR	A	B
Plagioclase - Quartz	0.97	$1.04 \cdot X_{An}$
Quartz - Biotite	3.69	-0.60
Plagioclase - Biotite	2.096	-0.60
Quartz - Water	4.10	-3.70

X_{An} = Anorthite content (for samples studied: JB 68 = 0.40; JB 105 = 0.60; JB 109 = 0.10)

Table 5: Factors used for calculating oxygen isotope temperatures from mineral pairs

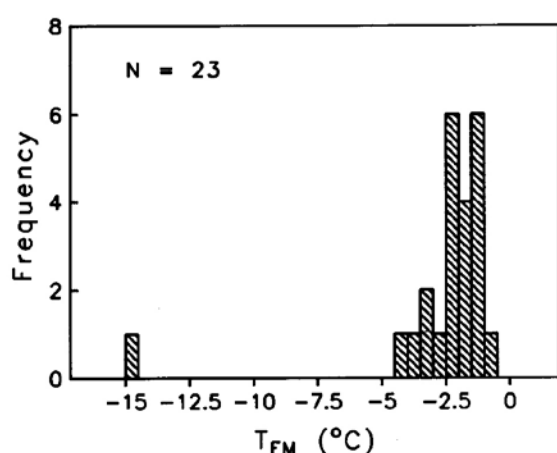


Figure 13: Histogram of final melting temperatures (T_m) for type A inclusions in quartz from vein sample HB004 (123)

SAMPLE	DESCRIPTION	$\delta^{18}O$ ‰	
		Quartz	Muscovite
HB 001 (300)	1 cm thick quartz-muscovite vein cutting quartz-sericite rock	10.4	6.8
HB 002 (22)	30 cm thick quartz-sulphide vein cutting medium- to fine-grained QFP	11.5	
HB 047 (287)	1 cm thick quartz-sulphide vein cutting QFP	9.8	
HB 072 (25.5)	80 cm thick quartz vein, with minor sulphide, cutting a fine-grained, dark coloured QP with euhedral pyrite	7.0	

Table 6: $\delta^{18}O$ data for vein minerals

the recognition of potassic hydrothermal alteration difficult. There is, however, some evidence for potassic alteration within the Haib QFP. Chlorite-sericite and quartz-sericite alteration of both the Haib QFP and the surrounding country rock are well developed, with the former hosting much of the high-grade copper mineralisation.

Rocks showing petrographic evidence for hydrothermal alteration are variably depleted in ^{18}O , as shown by low $\delta^{18}O$ values, pointing to exchange with isotopi-

SYSTEM	T_{IM} °C	T_{FM} °C	T_H °C
$H_2O - NaCl$	-19.6	-1.8	319 -L
	-21.5 to -19.7	?	120 -L
	-20.8 to -19.5	-1.3	?
	-22.1 to -20.3	-3.2	?
$H_2O - NaCl - KCl$	-24.3 to -24.0	-1.1	317 -L
$H_2O - NaCl - MgCl_2$	-37.3 to -36.5	-14.6	?

Table 7: Temperatures estimated from fluid inclusion microthermometry. Type A inclusions only. T_{IM} = temperature of initial melting, T_{FM} = temperature of final melting, T_H = temperature of homogenisation, "?" means T_H was too high to be measured by the apparatus used

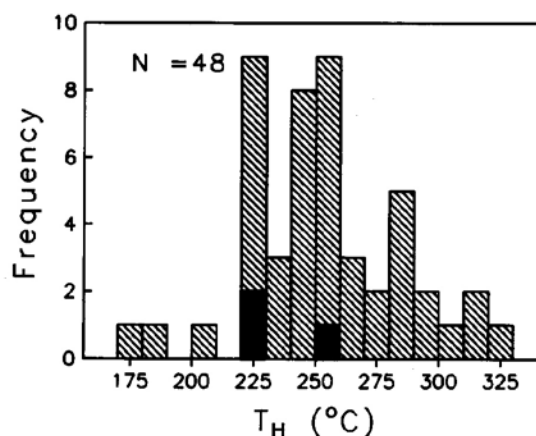


Figure 14: Histogram of homogenisation temperatures (T_H) for three Type C inclusions (solid) and forty-five Type A inclusions (hatch), in quartz from vein sample HB004 (123)

cally light: heated meteoric fluids. The little δD data so far obtained confirms the role of meteoric water, with altered rocks showing depletion in Deuterium. The patterns of $\delta^{18}O$ and δD variation observed in and around the Haib QFP are typical of other well-characterised hydrothermally altered granitoids and hydrothermal ore deposits. Features already recognised as comparing closely to Phanerozoic porphyry-type copper deposits are augmented by the isotopic evidence for hydrother-

mal convection cells developed as a result of intrusion and cooling of the Haib QFP. Finally, there appears to be some evidence for at least two generations of hydrothermal fluids in the history of the Haib deposit, with an early, high-temperature, high-salinity fluid present during emplacement of quartz-sulphide veins, followed by a later, lower temperature, low-salinity fluid trapped in healed fractures.

Acknowledgements

The Geological Survey of Namibia and its previous director R. McG. Miller are thanked for arranging financial support from the Committee for Research Priorities. Mr George Swanson, of Swanson Enterprises, Springbok, is thanked for access to the property and permission to sample the core. Torsten Vennemann and Chris Harris provided instruction on the use of the Stable isotope facilities at UCT. Chandra Mehl provided assistance in mineral separation and Stable isotope analysis. Fluid inclusion analysis at Wits was made possible through the efforts of Rudi Boer, Laurence Robb and Mike Meyer. Hydrogen isotope data was kindly supplied by Torsten Vennemann at the University of Michigan. Reviews by Drs Laurence Robb and Brian Hoal helped improve earlier versions of the manuscript.

References

- Blignault, H.J. 1977. Structural-metamorphic imprint on part of the Namaqua Mobile Belt in South West Africa. *Bull. Precamb. Res. Unit. Univ. Cape Town*, **23**, 197p.
- Blignault, H.J., Van Aswegen, G., Van Der Merwe, S.W. and Colliston, W.P. 1983. The Namaqua geotraverse and environs: part of the Proterozoic Namaqua mobile belt. *Spec. Publ. geol. Soc. S. Afr.*, **10**, 1-29.
- Bottinga, P. and Javoy, M. 1974. Oxygen isotope geothermometry of igneous and metamorphic rocks. *Trans. Am. Geophys. Un.*, **55**, 477.
- Bowles, M. 1988. Tungsten mineralisation in the Namaqualand - Bushmanland region, north-western Cape, South Africa. *Mem. geol. Surv. S. Afr.*, **74**, 102p.
- Burnham, C.W. 1962. Facies and types of hydrothermal alteration. *Econ. Geol.*, **57**, 768-784.
- Criss, R.E. and Taylor, H.P. 1986. Meteoric - hydrothermal systems. In: Valley, J.W., Taylor, H.P. and O'Neil, J.R. (Editors) *Stable isotopes in high temperature geological processes*. Reviews in Mineralogy, **16**, 373-424.
- De Villiers, J. and Söhnge, P.G. 1959. The geology of the Richtersveld. *Mem. geol. Surv. S. Afr.*, **48**, 295p.
- Ferry, J.M. 1985. Hydrothermal alteration of Tertiary igneous rocks from the Isle of Skye, Northwest Scotland. *Contrib. Mineral. Petrol.*, **91**, 283-304.
- Gevers, T.W., Partridge, F.C. and Joubert, G.K. 1937. The pegmatite area south of the Orange River in Namaqualand. *Mem. geol. Surv. S. Afr.*, **31**, 180p.
- Guilbert, J.M. and Park, C.P. 1986. *The geology of ore deposits*. W.H. Freeman, New York, 985p.
- Gustafson, L.B. 1978. Some major factors of porphyry copper genesis. *Econ. Geol.*, **73**, 600-607.
- Ikin, N.P. and Harmon, R.S. 1984. Tectonic history of the ophiolitic rocks of the Highland Border fracture zone, Scotland: Stable isotope evidence from rock-fluid interactions during obduction. *Tectonophysics*, **106**, 31-48.
- Keyser, T.K. 1986. Stable isotope variations in the mantle. In: Valley, I.W., Taylor, H.P. and O'Neil, J.R., Eds. *Stable isotopes in high temperature geological processes*. Reviews in Mineralogy, **16**, 141-164.
- Minnitt, R.C.A. 1979. *The geological setting of porphyry type copper mineralization in the Haib River area, South West Africa*. Unpubl. PhD thesis, Univ. of the Witwatersrand, 366p.
- Minnitt, R.C.A. 1986. Porphyry copper-molybdenum mineralization at Haib River, S.W. Africa. *Min. Deposits of SA, Geol. Soc. S. Afr.*, Vol. **11**, 1567-1585.
- Reid, D.L. 1977. Geochemistry of Precambrian igneous rocks in the lower Orange River Region. *Bull. Precamb. Res. Unit, Univ. Cape Town*, **22**, 397 pp.
- Reid, D.L. 1979a. Age relations within the mid-Proterozoic Vioolsdrif batholith, lower Orange River region. *Trans. geol. Soc. S. Afr.*, **82**, 305-311.
- Reid, D.L. 1979b. Petrogenesis of calc-alkaline metalavas in the mid-Proterozoic Haib Volcanic Subgroup, Lower Orange River region. *Trans. geol. Soc. S. Afr.*, **82**, 109-131.
- Reid, D.L. 1979c. Total rock Rb-Sr and U-Th-Pb isotopic study of Precambrian metavolcanic rocks in the lower Orange River region. *Earth Planet. Sci. Lett.*, **42**, 368-378.
- Reid, D.L. 1982. Age relationships within the Vioolsdrif batholith, lower Orange River region. II. Two stage emplacement history and the extent of Kibaran overprinting. *Trans. geol. Soc. S. Afr.*, **85**, 105-110.
- Reynolds, T.J. and Beane, R.E. 1985. Evolution of hydrothermal fluid characteristics at the Santa Rita, New Mexico, porphyry copper deposit. *Econ. Geol.*, **80**, 1328-1347.
- Sheppard, S.M.F. 1986. Characterisation and isotopic variations in natural waters. In: Valley, J.W., Taylor, H.P. and O'Neil, J.R., Eds. *Stable isotopes in high temperature geological processes*. Reviews in Mineralogy, **16**, 165-184.
- Smalberger, J.M. 1975. A history of copper mining in Namaqualand. C. Struik (Pty) Ltd, Cape Town, 152p.
- Thornton, C.P. and Tuttle, O.F. 1960. Chemistry of igneous rocks, I. Differentiation Index. *Amer. J. Sci.*, **258**, 664-684.
- Vennemann, T.W. and Smith, H.S. 1990. The rate and temperature of reaction of CIF₃ with silicate minerals, and their relevance to oxygen isotope analysis.

- Chem. Geol.*, **86**, 83-88.
- Viljoen, R.P., Minnit, R.C.A. and Viljoen, M.J., 1986. Porphyry copper-molybdenum mineralisation at the Lorelei, S.W.A./Namibia. *Min. Deposits of S.A. Geol. Soc. S. Afr.*, Vol. **11**, 1559-1566.
- Van Aswegen, G. 1988. *The evolution of the Proterozoic gneisses and other metamorphites in the Namqualand Traverse between Springbok and Vioolsdrif, South Africa*. Unpubl. Ph.D. Thesis, University of the Orange Free State, 450p.
- Yon Backstrom, J.W. and De Villiers, J. 1972. The geology along the Orange River between Onseepkans and the Richtersveld. Explanation Sheets 2817D (Vioolsdrif), 2818C and 0 (Goodhouse) and 2819C (Onseepkans). *Geol. Surv. S. Afr.*, 101p.
- Wenner, D.O. and Taylor, H.P. 1976. Oxygen and hydrogen isotope studies of a Precambrian granite-rhyolite terrane, St. Francois Mts., S.E. Missouri. *Bull. geol. Soc. Am.*, **87**, 1587-1598.